JOURNAL OF MAGNETIC RESONANCE 60, 66–78 (1984)

An Electron Spin-Echo Envelope Modulation Study of ^{14}N Nuclear Hyperfine and Quadrupole Coupling in Copper(II)/Nickel(II) Bis(*N*,*N*-di-*n*-butyl-dithiocarbamate)

E. J. REIJERSE, M. L. H. PAULISSEN, AND C. P. KEIJZERS

Department of Molecular Spectroscopy, University of Nijmegen, Toernooiveld, 6525 ED Nijmegen, The Netherlands

Received April 24, 1984

The electron spin-echo envelope modulation technique (ESEEM) is used to determine the ^{14}N hyperfine and quadrupole tensors in copper-doped nickel(II) bis(*N*,*N*-di-*n*-butyl-dithiocarbamate). The line positions and peak intensities of the Fourier-transformed ESEEM spectra are interpreted using simulated spectra, obtained by diagonalizing the full spin-Hamiltonian matrix. The ^{14}N quadrupole tensor can be accounted for theoretically by extended Hückel molecular orbital calculations. For the interpretation of the ^{14}N hyperfine tensor, however, an unrestricted molecular orbital calculation is necessary. Therefore, one should be cautious in drawing conclusions about spin-density distributions from small hyperfine couplings of nuclei in higher coordination spheres.

It is well known that the amplitude of the electron spin echo can show a periodic variation superimposed on the relaxation decay (*1*). This modulation effect is caused by magnetic interactions between the electron spins and nuclear spins involving in general (a) hyperfine interactions (HFI), (b) nuclear Zeeman interactions (NZI), and (c) nuclear quadrupole interactions (NQI). The modulation frequency and amplitude depend on the magnitude of these interactions. By Fourier transformation of the echo envelope one obtains Fourier-transformed electron spin-echo envelope modulation spectra (FT-ESEEM spectra) from which the interactions can be determined, thus offering an alternative to conventional ENDOR (*2*). One attractive feature of the FT-ESEEM spectrum is that its intensities depend only on the spin Hamiltonian of the system and not, as in cw-ENDOR, on any relaxation rate. Therefore, the FT-ESEEM intensities can be calculated in a straightforward manner (*3*).

A necessary condition for the observation of the modulation effect is that the spin states of the system are mixed; i.e., during the excitation of the system by a microwave pulse both first-order "allowed" and "forbidden" transitions must occur simultaneously inducing a "branching" over the $M_s = +1/2$ and $M_s = -1/2$ manifolds. This requires HFI and/or NQI of the same order of magnitude as the NZI. In many systems which do have a NQI, this interaction turned out to be much smaller than the NZI and the HFI. In most of these cases it was neglected completely to obtain analytical expressions for the modulation pattern (*3, 4*). Only in a few instances was the NQI taken into account as a perturbation which affects only the amplitude of the modulations (*5*). However, we are interested in various

0022-2364/84 $3.00

Jahn–Teller systems with nitrogen-containing ligands (*6*). Because the nitrogen atoms are in the second coordination sphere, it is to be expected that their HFI and most probably also their NQI are of the same order of magnitude as the NZI. Therefore, in these systems we had no other alternative than to diagonalize the complete spin-Hamiltonian matrix and to make use of the exact modulation formula (*3*).

Since these Jahn–Teller systems contain at least three sets of two equivalent nitrogen atoms, which gives rise to very complicated spectra, we decided to measure first a system with only one set of equivalent nitrogen molecules but with HFI and NQI which are expected to be of the same order of magnitude as the NZI. For this model system, we have chosen copper(II)/nickel(II) bis(*N*,*N*-di-*n*-butyl-dithiocarbamate) (Cu/Ni(bu_2dtc)$_2$) because much is known already about its electronic structure from EPR and ENDOR measurements and various molecular orbital (MO) calculations (*7–10*).

EXPERIMENTAL

The 1% Cu-doped Ni(bu_2dtc)$_2$ crystals were grown by slow evaporation of an acetone solution that contained the two complexes in the appropriate ratio.

Field swept spectra were measured by continuously monitoring the intensity of a two-pulse echo (pulse sequence: $\pi/2$–τ–π–τ–echo, i.e., two microwave pulses separated by time τ) while sweeping the magnetic field. These spectra are equivalent to a conventional cw-EPR spectrum in absorption mode.

The ESEEM spectra were measured using the stimulated echo sequence ($\pi/2$–τ–$\pi/2$–T–$\pi/2$–τ–echo) which consists of three equal pulses (*11*), and sweeping time T between the second and the third pulse. For τ, a constant value of 300 ns was used. T was swept from 1 to 51 μs in steps of 0.1 μs. The repetition time was 10 ms.

All measurements were carried out at a temperature of 15 K in an Oxford CF200 liquid helium flow cryostat with two orthogonal rotation axes (one inside the stripline resonator ($Q \sim 100$ (12)) and one being the cavity itself).

The microwave pulses had a length of 20 ns and were generated by a home-built programmable pulse generator with a time resolution of 10 ns. They were amplified by a 1 kW Litton TWT amplifier. The electron spin echoes were sampled and integrated in a boxcar PAR 162/164. The data were collected and processed in a MINC 11/23 minicomputer with home-written software. The modulation envelopes were transformed into the frequency domain using standard procedures: high-pass filtering (cut-off frequency 50 kHz), Fourier transformation, and transformation to amplitude mode. The microwave frequency was measured with a Hewlett–Packard 5246L counter, equipped with a 5255A plug-in unit. The magnetic field was monitored with a Bruker B-NM12 gauss meter.

RESULTS

Determination of the Nitrogen Interactions

Figure 1 shows a typical field-swept spectrum. The host crystal has space group $P2_{1/c}$, with two magnetically nonequivalent molecules per unit cell. Since the

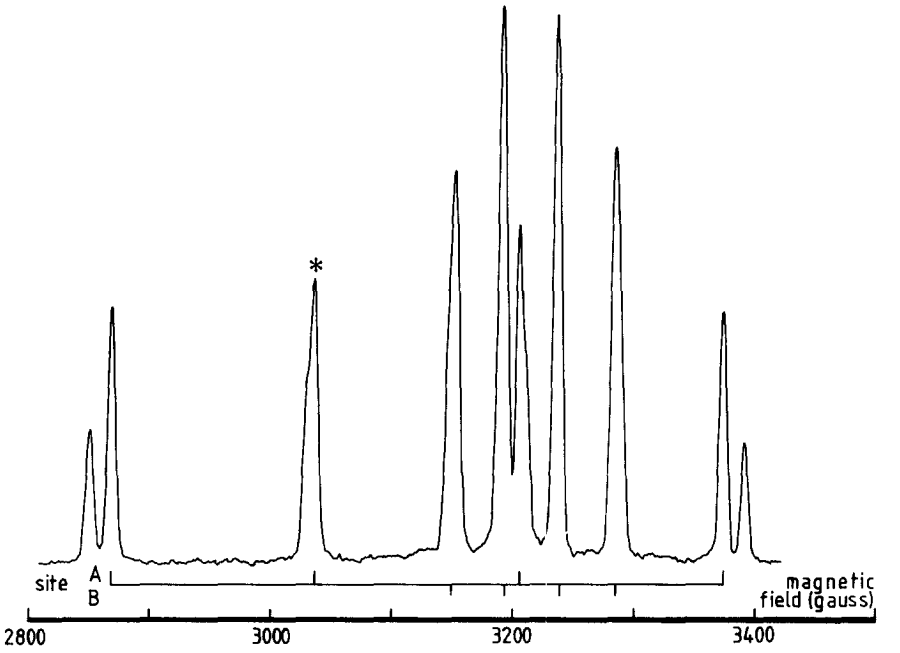

FIG. 1. Field-swept spectrum of 1% Cu doped $Ni(bu_2dtc)_2$ in the *YZ* plane. Angle with *Y* axis = 80°, τ = 300 ns.

copper-containing molecules accept the structure of the nickel complex (*10, 14*), this gives rise to two copper hyperfine quartets (except when the magnetic field is along the *b* axis or in the *ac* plane). All lines are partly split due to the naturally occurring ^{63}Cu and ^{65}Cu isotopes, each with a nuclear spin 3/2 but with a slightly different magnetic moment. From these field-swept ESE spectra we determined the *g*, the Cu-HFI, and the Cu-NQI tensors. The principal values are listed in Table 1. The principal axes of the *g* tensor are indicated in Fig. 2. They were chosen as the axes of rotation in the determination of the ^{14}N coupling tensors. The maximum *g* value and the maximum copper HFI coincide along the normal to the molecular plane. In the plane, both tensors are almost axial. Surprisingly, the HFI tensor has been rotated by 29° relative to **g**. However, one should bear in mind that the error in the in-plane angle is quite large because of the mentioned near axiality. The Cu NQI is very small compared to the Cu HFI. Its maximum value coincides with the maximum Cu HFI and the maximum *g* value along the normal to the molecular plane. However, the NQI tensor is clearly nonaxial, as opposed to the other two tensors.

The ESEEM spectra were recorded by pulsing on one of the copper-hyperfine lines of one site (marked with an asterisk in Fig. 1). In Fig. 3 a typical ESEEM spectrum is shown; the filtered signal and the FT spectrum are also presented. The angular dependence of the FT-ESEEM spectra in the *YZ* plane of the molecule is shown in Fig. 4. From the comparison of these FT-ESEEM spectra with some spectra measured for the analogous ethyl complex, we concluded that only the shaded peaks are due to ^{14}N coupling in the complex. The other signals most

TABLE 1

Measured and Calculated S Hyperfine, ^{63}Cu Hyperfine, and Quadrupole Interaction Tensors (in Units of 10^{-4} cm^{-1}) and g Tensor of Cu/Ni(R_2dtc)$_2$ Complexes

	Measured		Calculated			
R:	n-Butyl	Ethyl	Ethyl	H	H	H
Temp:	15 K	25 K				
Method:	ESE	ESR[a]	EH[b]	EH[c]	UHFS[d]	RHFS[d]
g_x	2.016	2.017	2.019	2.020	2.029	2.029
g_y	2.023	2.020	2.024	2.025	2.037	2.039
g_z	2.084	2.084	2.074	2.078	2.116	2.114
Cu-A_1	43.8 [29][e]	42.6	39.6	40.6	44.3	38.5
A_2	39.9 [29][e]	41.4	38.9	39.9	45.0	41.1
A_z	−83.7 [1][e]	−84.0	−78.6	−80.5	−89.3	−79.6
A-iso	−81.7	−84.5	0.0	0.0	−56.9	22.9
Cu-P_x	−0.9 [2][e]		−1.4	−1.4		
P_y	−0.3 [2][e]		−1.3	−1.3		
P_z	1.2 [2][e]		2.7	2.8		
S-A_1		10.2	10.4	10.3	7.8	7.8
A_2		−5.9	−5.1	−5.1	−4.0	−3.9
A_3		−4.3	−5.2	−5.2	−3.8	−3.9
A-iso		11.6	11.3	11.7	17.0	12.2

[a] g tensor and copper data obtained from ref. (*10*). Sulphur data obtained from Ref. (*16*).
[b] Data based on EH calculations of Ref. (*9*) with ethyl groups retained.
[c] Data based on EH calculations of Ref. (*9*) with ethyl groups replaced by protons.
[d] Data obtained from Ref. (*8*).
[e] Angle of the principal axis with the corresponding one of the g tensor.

probably originate from strong couplings with protons of neighbor molecules. From the line positions in the three measured planes (depicted in Fig. 5), it can easily be concluded that the ^{14}N coupling tensors are almost axial in the XY plane. This gave a clue to the assignment of the peaks in the spectra: model calculations could be restricted to axial and coinciding HFI (A^N) and NQI (P^N) tensors. They led to the assignment of the peaks as indicated in Fig. 5. The corresponding energy-level diagram for the orientation of the ESEEM spectrum in Fig. 3 is given in Fig. 6. Because the two ^{14}N atoms in the complex are equivalent, all line positions in Fig. 5 were fitted to this six-level scheme of one electron and one ^{14}N nucleus. The introduction of the second ^{14}N spin results only in small splittings of the ^{14}N lines

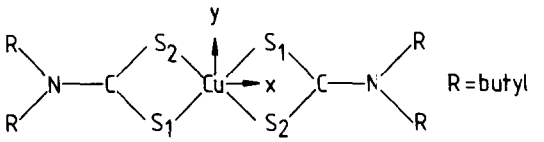

FIG. 2. Orientation of the principal axes of g (tensor) in Cu/Ni(bu_2dtc)$_2$.

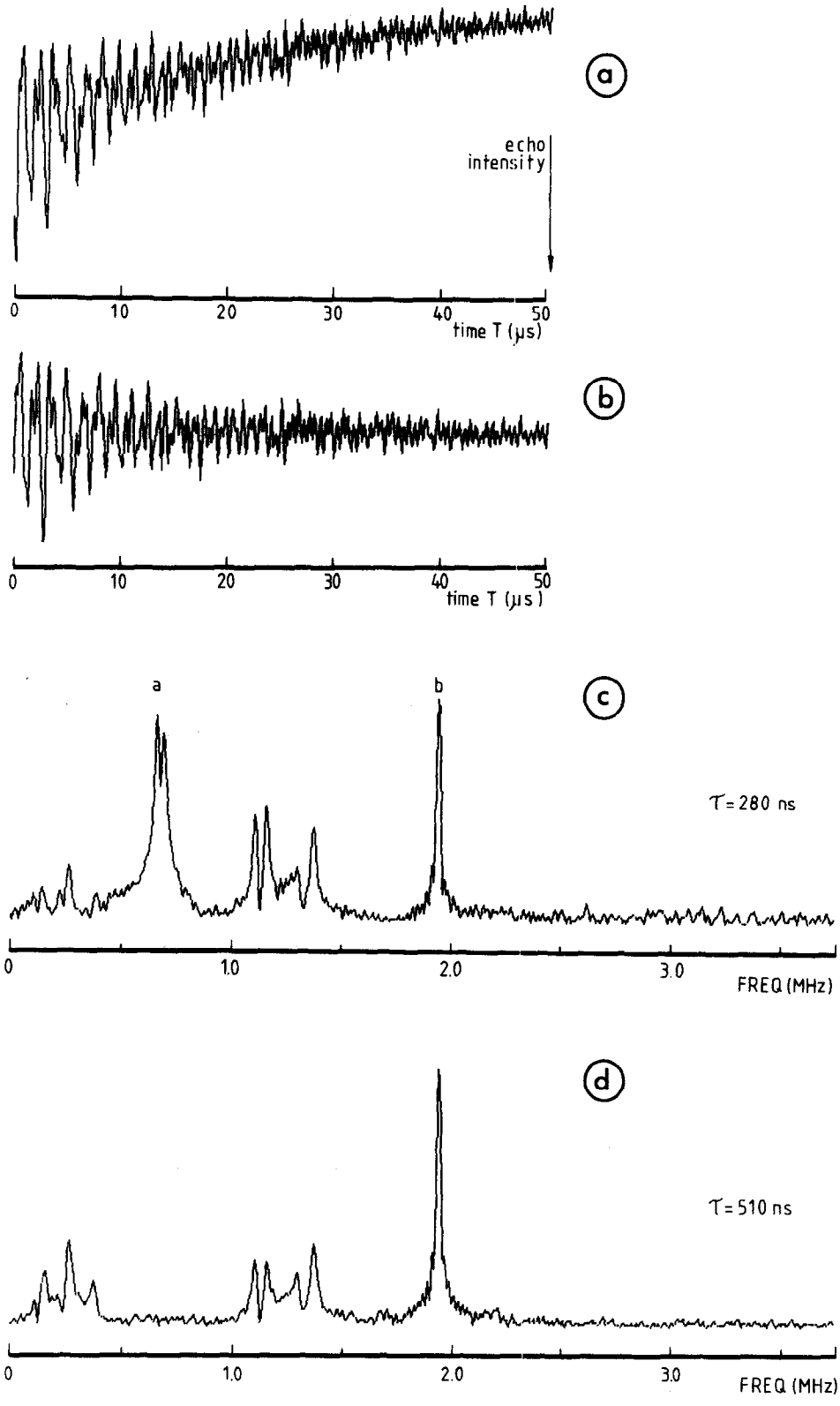
a
echo
intensity
0
10
20
30
40
50
time T (μs)
b
0
10
20
30
40
50
time T (μs)
a
b
c
τ = 280 ns
0
1.0
2.0
3.0
FREQ (MHz)
d
τ = 510 ns
0
1.0
2.0
3.0
FREQ (MHz)

which splittings are, albeit observable in the spectra (e.g., peak a in Fig. 3c), too small to affect the fit of the ^{14}N interaction tensors. Further refinement was accomplished by relaxing the restrictions of axial and coinciding nitrogen tensors and by including the g and Cu-HFI tensors. The resulting nitrogen tensors are presented in Table 2. As expected, they are almost axial in the XY plane. The HFI is dominated by its isotropic part, which is three times as large as the anisotropic contribution. Along the principal axis, perpendicular to the molecular plane, the HFI and the NQI are almost equal ($\sim 0.5 \times 10^{-4}$ cm^{-1}) and of the same order of magnitude as the nuclear Zeeman interaction ($\sim 0.3 \times 10^{-4}$ cm^{-1}). This prevented the use of approximate formulae for the modulation pattern, as was mentioned above. By fitting the FT-ESEEM spectra we could not distinguish the absolute or relative signs of the interactions; the signs listed in Table 2 are based on theoretical calculations (see below).

Intensities of the Spectra

To check the reliability of the measured tensors we calculated the modulation intensities with the general equations derived by Mims (*3*). The intensity of a three-pulse echo is a function of time τ between the pulses 1 and 2, and time T between the pulses 2 and 3; apart from relaxation effects and instrumental properties, it is given by the following equation:

$$E_\tau(T) = \chi_0 + \frac{1}{2}\sum_{i>j}\chi_{ij}\cos\omega_{ij}\tau + \frac{1}{2}\sum_{k>n}\chi_{kn}\cos\omega_{kn}\tau + \sum_{i>j}\cos\omega_{ij}(T+\tau)$$
$$\times\left(\frac{1}{2}\chi_{ij} + \sum_{k>n}\chi_{ij,kn}\cos\omega_{kn}\tau\right) + \sum_{k>n}\cos\omega_{kn}(T+\tau)\left(\frac{1}{2}\chi_{kn} + \sum_{i>j}\chi_{ij,kn}\cos\omega_{ij}\tau\right) \quad [1]$$

where $i \neq j$ and $k \neq n$ and indices i, j run over the spin states within the electron spin manifold $M_s = -1/2$, while k, n run over the states of electron spin manifold $M_s = +1/2$. The quantity ω_{ij} is the energy difference (in rad s^{-1}) between the i and j spinstate. The terms in Eq. [1] which describe the amplitudes of the modulations have the following form:

$$\chi_0 = \left[\frac{1}{2I+1}\right]\sum_{i,k}|M_{ik}|^4 \quad [2]$$

$$\chi_{ij} = \left[\frac{2}{2I+1}\right]\sum_{k}|M_{ik}|^2|M_{jk}|^2 \quad [3]$$

$$\chi_{kn} = \left[\frac{2}{2I+1}\right]\sum_{i}|M_{ik}|^2|M_{in}|^2 \quad [4]$$

FIG. 3. (a) Typical ESEEM signal measured on the second peak of site A at the same orientation as in Fig. 1, τ = 280 ns. (b) Corresponding filtered signal (cutoff frequency = 50 kHz). (c) FT-ESEEM spectrum, 1000 points, Fourier transform of signal in Fig. 3b. (d) FT-ESEEM spectrum, 1000 points, τ = 510 ns, same orientation. The choice of τ = 510 ns ($1/\tau$ = 1.9 MHz) suppresses the corresponding frequency of peak b in the other M_s manifold (apparently peak a).

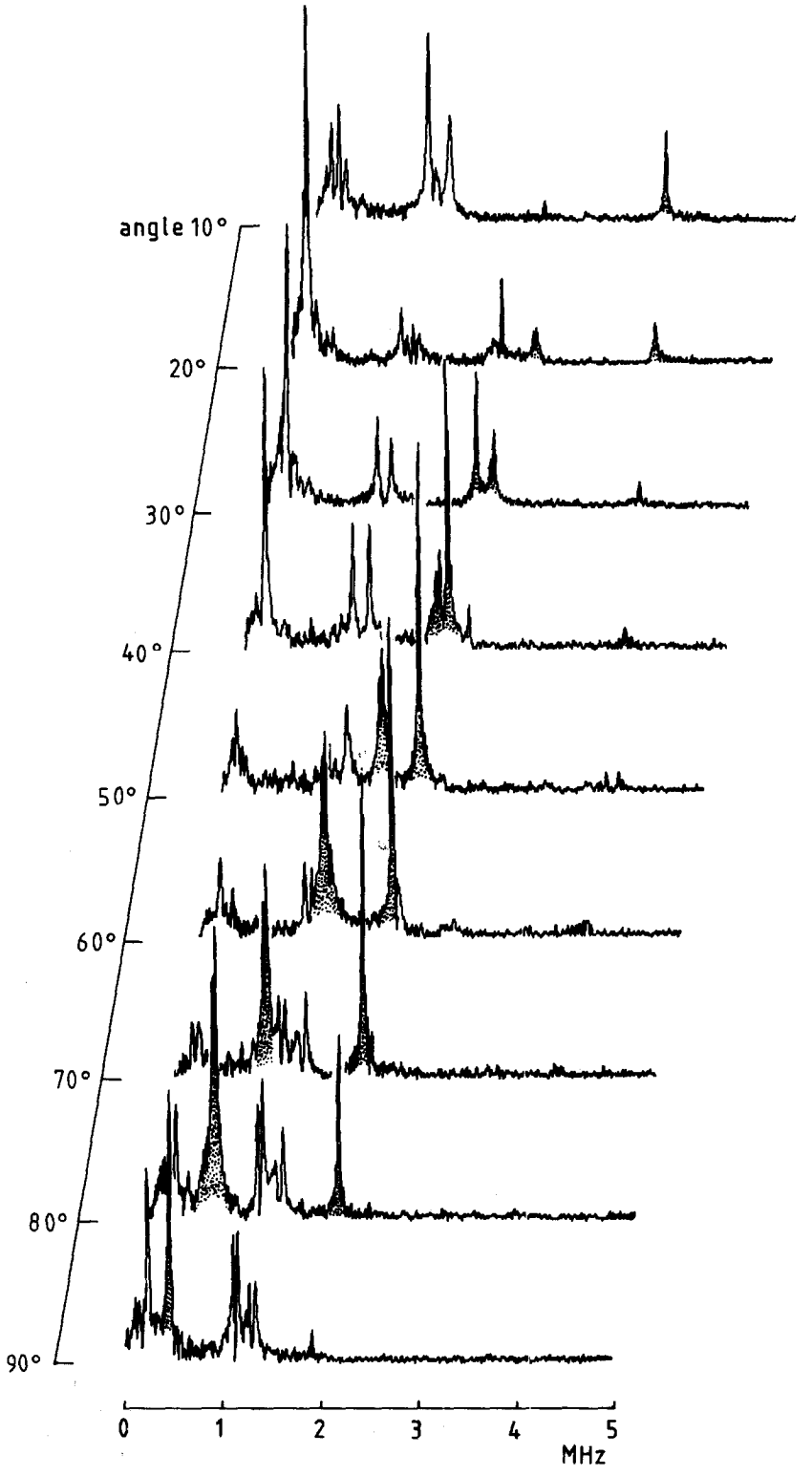

FIG. 4. Angular dependence of FT-ESEEM spectra in the *YZ* plane.

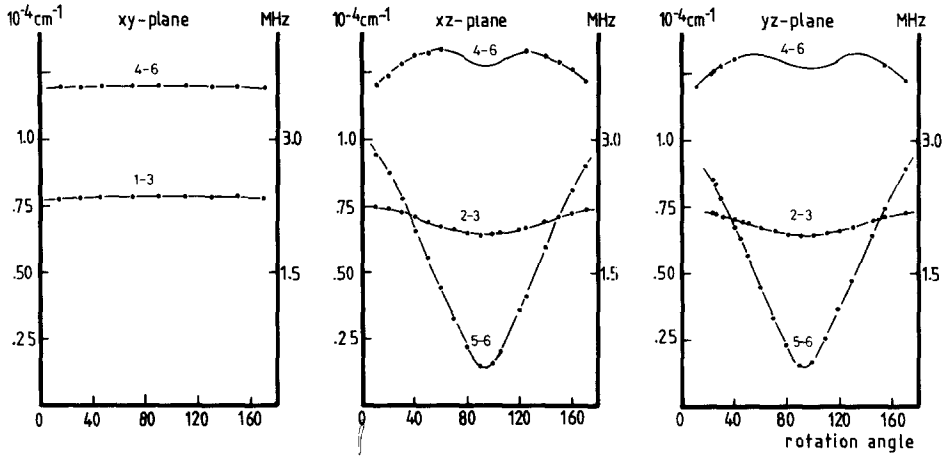

FIG. 5. Line positions of FT-ESEEM spectra in three planes.

$$\chi_{ij,kn} = \left[\frac{2}{2I+1}\right] \mathrm{Re}(M^*_{ik}M_{in}M^*_{jn}M_{jk}). \qquad [5]$$

M_{ik} are the elements of a unitary state-mixing matrix with dimension $2I + 1$; they can be referred to as the EPR transition moments from state i to state k. The transition moments can be calculated from the eigenvectors of the Hamiltonian (*3*). From this equation it is clear that the amplitude of the modulation at frequency ω_{ij}, is modulated with frequency ω_{kn} from the other M_s manifold and vice versa. By chosing appropriate values for τ, one is able to suppress or enhance the amplitude of frequencies of the *opposite* manifold. Complete suppression can occur when $\chi_{i,j} = \chi_{k,n}$, $\chi_{ij,kn} = -(1/2)\chi_{k,n}$ (which appeared to be the case for our spin Hamiltonian) and τ is chosen such that it is a multiple of $2\pi/\omega_{ij}$ or $2\pi/\omega_{kn}$. In this way one can use the suppression effect to assign modulation frequencies to different M_s manifolds. This is demonstrated in Figs. 3c and d where peaks a and b are assigned to different M_s manifolds. The calculated intensities for the three-pulse ESEEMs with τ = 300 ns are plotted as a function of the angle in the YZ plane in Fig. 7. In the calculation we used a spin Hamiltonian with one electron spin $S = 1/2$, and two ^{14}N nuclear spins $I = 1$; the Cu spin $I = 3/2$ was omitted as it turned out to have hardly any influence. It should be noticed, however, that for the calculation of the line positions (vide supra) only one of the two equivalent ^{14}N nuclear spins was taken into account. The introduction of the second (equivalent) ^{14}N spin led only to small splittings in the ^{14}N line positions but, more important, it leads also to an increase of the calculated intensities by a factor of 1.7 as compared to the one-^{14}N spin case. In principle it is possible to determine the "normalized" modulation intensities (relative to the echo intensity) from the spectra (*13*). However, the overlap with proton signals, the mentioned splittings of the ^{14}N signals and the limited S/N ratio prevented us from obtaining reliable intensity data from the spectra, but as can be judged from a comparison of Figs. 4 and 7, the overall correspondence of the calculated intensities and the experimental data is very good.

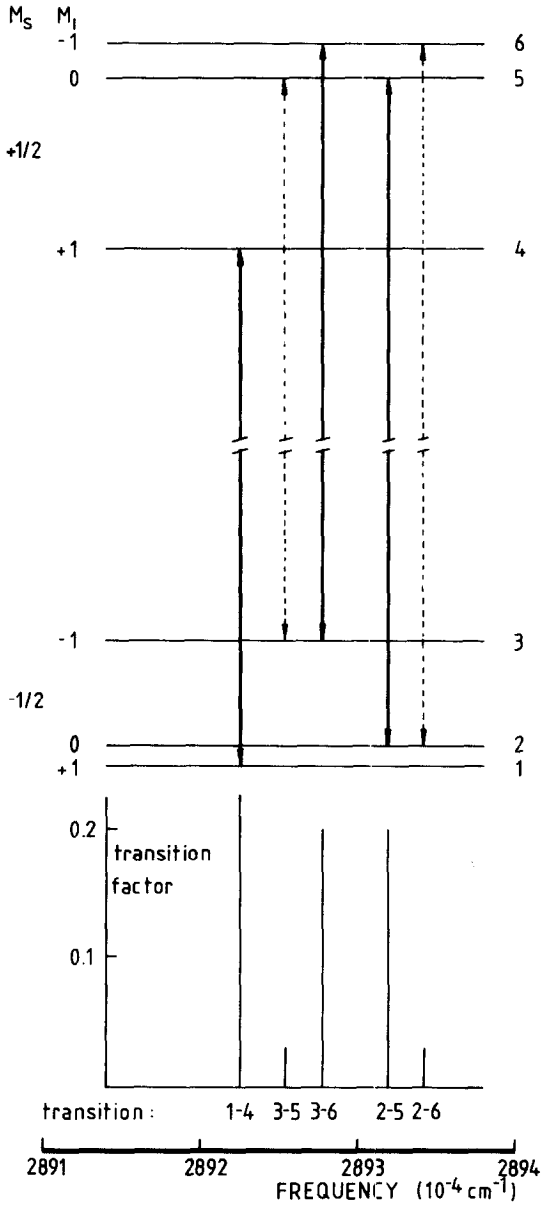

FIG. 6. Calculated energy-level diagram using a spin Hamiltonian with one electron spin $S = 1/2$ ($g = 2.032$) and one ^{14}N nuclear spin $I = 1$ with the hyperfine interaction and quadrupole interaction of Table 2 for the orientation of Fig. 1.

DISCUSSION

The g tensor and the Cu-HFS data are in agreement with the data of Weeks and Fackler (*14*) and Snaathorst *et al.* (*10*) for the ethyl complex. The ^{14}N data can only be compared with the ENDOR studies by Kirmse *et al.* (*15*), also for the ethyl

TABLE 2

Measured and Calculated ^{14}N-Hyperfine and Quadrupole Interaction Tensors in $Cu/Ni(R_2dtc)_2$ Complexes (in Units of 10^{-4} cm^{-1})

			Calculated							
	Measured		1-center				2 + 3-center	1 + (2 + 3)center[f]		
R:	*n*-Butyl	Ethyl	Ethyl	H	H	H	H			
Temp:	15 K	27.3 K								
Method:	FT-ESEEM	ENDOR[a]	EH[b,g]	EH[c,g]	RHFS[d]	URHF[d]	EH[e]	EH	RHFS	UHFS
N-A_x	0.06		−0.01	−0.01	−0.03	0.08	0.05	0.04	0.02	0.13
A_y	0.06		0.02	0.02	0.05	0.16	−0.01	0.01	0.04	0.15
A_z	−0.12 [2][h]		−0.01	−0.01	−0.03	−0.24	−0.04	−0.05	−0.07	−0.28
A-iso	−0.375	0.50	0.0	0.0	0.0	−0.56	0.0	0.0	0.0	−0.56
N-P_x	0.24		0.55	0.66						
P_y	0.23		0.46	0.41						
P_z	−0.47 [3][h]	0.35 [17][h]	−1.01	−1.07						

[a] Data obtained from Ref. (*15*).
[b] Data based on EH calculations from Ref. (*9*), with full ethyl groups retained.
[c] Data based on EH calculations from Ref. (*9*), with ethyl groups replaced by protons.
[d] Data obtained from Ref. (*8*).
[e] Data obtained from Ref. (*9*).
[f] 1-center contribution from method mentioned. (2 + 3)-center from EH method of Ref. (*9*).
[g] The 1-center contributions calculated with the EH method include first- and second-order contributions.
[h] Angle of the principal axis with the corresponding one of the g tensor.

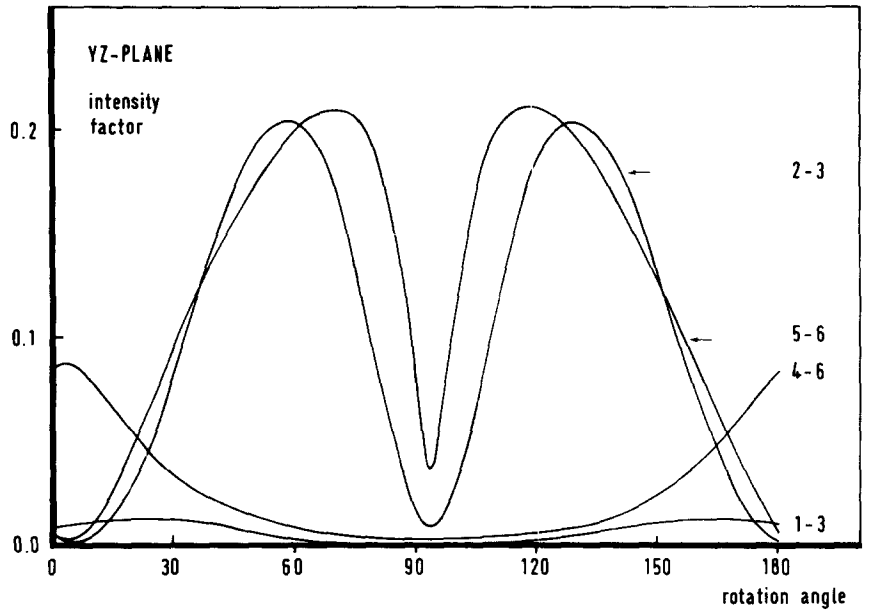

FIG. 7. Calculated three-pulse FT-ESEEM intensities (τ = 300 ns) in the YZ plane; the numbering of the energy levels is according to Fig. 6. 4° = Y axis; 94° = Z axis.

complex. Because the ENDOR signals were too weak for a full rotational study, only approximate values could be obtained; these are listed in Table 2. Their data show some deviations from ours: In our study both the maximum P^N and A^N direction coincide with the maximum g direction, while the study of Kirmse *et al.* indicates for the P_{max} direction a deviation of 17 ± 5° from the molecular axis system (Fig. 2); both, the estimated A^N-iso and the P^N_{max} values show a deviation of ~25% from our values. On the other hand, the estimated order of magnitude of 0.1×10^{-4} cm^{-1} for the dipolar part of the ^{14}N hyperfine interaction, agrees with our experimental result.

Several studies have been made to calculate the magnetic coupling parameters of Cu/Ni(et$_2$dtc)$_2$ (*7–9*). The most recent calculation (*9*) included two- and three-center contributions to the first-order anisotropic HFI. The second-order HFI is generally rather small, and two- and three-center integrals are, therefore, neglected. The first-order contribution is brought about by the electron spin–nuclear spin dipole–dipole interaction (e.g., with nucleus N) and can be expressed as

$$A^N_{ij} = \left(\frac{\mu_0}{4\pi}\right) g_e g_N \mu_b \mu_n \left\langle \psi_0 \left| \frac{F^N_{ij}}{r^3_N} \right| \psi_0 \right\rangle \qquad [6]$$

where μ_0 is the permeability of free space, μ_b is the Bohr magneton, g_e the free-electron g value, and g_N the gyromagnetic ratio of nucleus N; i, j are x, y, z, F^N_{ij} is a component of a symmetrical traceless tensor operator related to the dipolar interaction and r_N is the electron–nucleus distance. If ψ_0, the molecular orbital of the unpaired electron, is expanded as a linear combination of atomic orbitals ϕ^A_i centered on nuclei A, then Eq. [6] can be rewritten

$$A_{ij}^{N} = \left(\frac{\mu_0}{4\pi}\right) g_e g_N \mu_b \mu_n \times \sum_A \sum_B \sum_{i \in A} \sum_{j \in B} \left\langle C_i^A \phi_i^A \left| \frac{F_{ij}^N}{r_N^3} \right| C_j^B \phi_j^B \right\rangle$$
$$= (A_{ij}^N)_1 + (A_{ij}^N)_{2,1} + (A_{ij}^N)_{2,2} + (A_{ij}^N)_3 \qquad [7]$$

where $(A_{ij}^N)_1$ and $(A_{ij}^N)_3$ are the one and three-center contributions, respectively. $(A_{ij}^N)_{2,1}$ and $(A_{ij}^N)_{2,2}$ are two-center contributions, $(A_{ij}^N)_{2,2}$ having one atomic orbital centered on nucleus N (A or B = N) and $(A_{ij}^N)_{2,1}$ having both orbitals centered on the same nucleus, not being N (A = B $\neq$ N). In Ref. (*9*), the hyperfine couplings were calculated with spin densities which were obtained from extended Hückel (EH) calculations in which the ethyl groups of the complex were replaced by protons. This reduces the computing time considerably but, since it is to be expected that this approximation will not be valid for the ^{14}N NQI, we used those EH data from Ref. (*9*) which were obtained by retaining the ethyl groups. The calculated first- and second-order one-center contributions to the hyperfine interactions of copper, sulfur, and nitrogen and to the quadrupole couplings of copper and nitrogen are summarized in Tables 1 and 2. The experimental g and the A^{Cu} and A^S tensors are in good agreement with the theoretical calculations, both with the semi-empirical extended Hückel (EH) method and with the ab initio Hartree–Fock–Slater (HFS) method. The picture that emerges from both methods is that the unpaired electron is located in the center of the molecule: ~50% on Cu and ~50% on the four sulfur atoms. The density on the other atoms is very small. It is, therefore, to be expected that the anisotropic dipolar part of the A^N tensor is dominated by two- and three-center interactions between the magnetic moment of the nitrogen nucleus and the unpaired electron on copper and sulfur (*9*). Hence, the main principal axis of A^N is expected to be located in the molecular plane, pointing from N to Cu (if the molecule has D_{2h} symmetry). Is was, therefore, very surprising that the axial component of A^N is not located along the X axis but, on the contrary, points along the Z axis, perpendicular to the molecular plane.

It turned out that the restricted MO methods (both EH and RHFS) could not explain this discrepancy. Both methods yield a one-center contribution which is axial along the Y axis (because of the fact that the unpaired electron is located in the p_y orbital of N, which orbital mixes with the $3d_{xy}$ orbital of Cu). The (2 + 3)-center contributions were calculated only from the spin densities which were obtained via the EH method with the same procedure as was used in Refs. (*9, 10*). From previous calculations of ^1H-hyperfine interactions in the same molecule, it was concluded that these multicenter terms are very accurate, notwithstanding the semi-empirical nature of this MO method (*9, 10*).

The multicenter contribution is of the same order of magnitude as the one-center term and far from axial: its minimum value is along Y, the direction of maximum one-center contribution! The total of the calculated A^N tensor has its maximum value along Z. The deviation from axial symmetry is much larger than in the experiment. The strongest discrepancy is, however, that the calculated isotropic part of the tensor is zero, as must be expected for an MO with b_{1g} symmetry. To explain the full tensor, we must turn to the results of unrestricted HFS calculations (*8*) (Table 2). They yield a one-center contribution which indeed has its main axis along Z and also has a large isotropic component. The correction with the (2 + 3)-

center contributions (from EH) results in a tensor which has the experimental symmetry but is too large. The latter must be caused by an overestimation of the very small spin-density on N.

The quadrupole-interaction tensor was calculated only with the EH method. Although it is too large, its symmetry is in perfect agreement with the experiment.

CONCLUSION

It is shown that in a transition-metal complex the magnetic interaction parameters of weakly coupled nuclei can be determined accurately by FT-ESEEM spectroscopy. Theoretically, however, these parameters can only be accounted for by unrestricted molecular orbital calculations. This implies that one has to be very careful in extracting information about chemical bonding from these experimental results.

ACKNOWLEDGMENTS

The authors gratefully acknowledge the indispensible technical support from Mr. Jan van Os and Mr. Adrie Klaassen who designed and built our electron spin echo spectrometer. Professor E. de Boer who initiated our activities in the field of ESE spectroscopy is thanked for critically reading the manuscript and for his continued interest. This work is financially supported by the Netherlands Foundation for Chemical Research (SON).

REFERENCES

1. L. G. ROWAN, E. L. HAHN, AND W. B. MIMS, *Phys. Rev. A* **137,** 61 (1965).
2. H. BARKHUYSEN, R. DE BEER, E. L. DE WILD, AND D. VAN ORMONDT, *J. Magn. Reson.* **50,** 299 (1982).
3. W. B. MIMS, *Phys. Rev. B* **5,** 2409 (1972); *Phys. Rev. B* **6,** 3543 (1972).
4. W. B. MIMS *in* "Electron Paramagnetic Resonance" (S. Geschwind, Ed.), Chap. 4, Plenum, New York, 1972.
5. A. A. SHUBIN AND S. A. DIKANOV, *J. Magn. Reson.* **52,** 1 (1983).
6. J. S. WOOD, C. P. KEIJZERS, E. DE BOER, AND A. BUTTAFAVA, *Inorg. Chem.* **19,** 2213 (1980).
7. C. P. KEIJZERS, H. J. M. DE VRIES, AND A. VAN DER AVOIRD, *Inorg. Chem.* **11,** 1138 (1972).
8. P. J. M. GEURTS, P. C. P. BOUTEN, AND A. VAN DER AVOIRD, *J. Chem. Phys.* **73,** 1306 (1980).
9. C. P. KEIJZERS AND D. SNAATHORST, *Chem. Phys. Lett.* **69,** 348 (1980).
10. D. SNAATHORST, C. P. KEIJZERS, A. A. K. KLAASSEN, E. DE BOER, V. P. CHACKO, AND R. GOMPERTS, *Mol. Phys.* **40,** 585 (1980).
11. E. L. HAHN, *Phys. Rev.* **80,** 580 (1950).
12. J. L. DAVIS AND W. B. MIMS, *Rev. Sci. Instrum.* **49,** 1095 (1978).
13. H. BARKHUYSEN, R. DE BEER, AND D. VAN ORMONDT, *Chem. Phys. Lett.* **101,** 494 (1983).
14. M. J. WEEKS AND J. P. FACKLER, *Inorg. Chem.* **7,** 2548 (1969).
15. R. KIRMSE, U. ABRAM, AND R. BÖTTCHER, *Chem. Phys. Lett.* **90,** 9 (1982).
16. R. KIRMSE AND B. V. SOLOVEV, *J. Inorg. Nucl. Chem.* **39,** 41 (1977).